

# Divergent Fluctuations from an Infrared 2D-Mode Catastrophe

Richard G. Hennig<sup>1,2</sup> and Clotilde S. Cucinotta<sup>3</sup>

<sup>1</sup>*Department of Materials Science, University of Florida, Gainesville, FL 32611, USA*

<sup>2</sup>*Quantum Theory Project, University of Florida, Gainesville, FL 32611, USA*

<sup>3</sup>*Department of Chemistry, Imperial College London, London, W12 0BZ, United Kingdom*

(Dated: January 15, 2026)

Molecular simulations of interfacial polar media routinely employ periodic boundary conditions parallel to the interface. We show that this geometry injects a uniform plane mode ( $q_{\parallel} = 0$ ) that converts the plane-averaged electrostatic potential into a cumulative sum of plane-dipole increments, a random walk in  $z$ . Consequently, the variance of the plane-averaged potential grows linearly with depth in semi-infinite slabs and follows a parabolic Brownian-bridge profile in finite cells with both ends fixed, with an amplitude inversely proportional to the cell's lateral area. Hence, at any finite area, the variance diverges with slab thickness—a 2D-mode catastrophe. In contrast, a pure 1D chain (no lateral replication) and a fully 3D, nonperiodic medium both exhibit bounded fluctuations that saturate with distance. The mechanism is generic to any solver of Poisson's equation with 2D periodicity, so the apparent growth and ultimate divergence in potential fluctuation are artifacts of boundary conditions rather than material response, and we provide a simple scaling criterion for choosing slab sizes that keeps these artifacts under quantitative control.

**Introduction**—Fluctuations of the electrostatic potential drive rates, selectivity, and stability across problems that span electrochemistry and molecular biology. In electrode–electrolyte systems, the variance and spectrum of the plane-averaged potential feed directly into key observables, including double-layer capacitance, the potential of zero charge, reorganization energies for electron transfer, ionic screening, interfacial and solvation free energies, and noise floors in nanoscale sensing [1–9]. In practice, these quantities are often obtained by laterally averaging charge or polarization and integrating the 1D Poisson equation in molecular simulations [10, 11].

In biomembranes and nanopores, the same plane-average workflow is used to reconstruct membrane potentials and gating charges [8–10]. Similar analyses appear in ferroelectric and piezoelectric thin films, polar 2D materials, and molecular electronics, where macroscopic boundary conditions set device-relevant internal fields [12]. At electrified metal–electrolyte interfaces, recent *ab initio* studies have resolved Pt–water double layers under bias [13–15] and developed constant-potential, open-boundary schemes for controlling electrode potential [16, 17]. In many of these settings, recent studies report large electrostatic potential fluctuations that persist over nanometer scales and argue that these fluctuations arise from collective electrostatic modes and from slow interfacial dynamics that directly influence the thermodynamics and kinetics of water and electrolytes [18, 19].

In this Letter we identify an infrared catastrophe of the uniform plane mode ( $q_{\parallel} = 0$ ), inherent to the planar electrostatic Green's function of 2D-periodic slabs, that causes an *apparent divergence* of plane-averaged potential fluctuations with slab thickness. Previous work on electrostatic boundary conditions and Poisson solvers in slab and interfacial geometries has focused primarily on obtaining accurate *mean* electrostatic potentials, fields, and

energies [20–25], whereas the impact of these choices on the *moments and cumulants* of the potential has received far less systematic attention—even though the variance directly enters thermodynamic and kinetic quantities such as free energies and rates [6, 7].

The uniform plane mode turns the plane-averaged electrostatic potential into a sum of independent (or weakly correlated) potential jumps—a random walk in  $z$ , so the variance grows linearly with depth (or parabolically across a finite slab), with a prefactor that decreases as the cell's lateral area  $A$  increases. The effect is most severe at small  $A$  and inflates response and rate estimates. In contrast, a pure 1D chain and fully 3D, nonperiodic media exhibit bounded fluctuations that saturate with distance. As with classic divergences—the ultraviolet catastrophe and Stokes' paradox—the growth found here reflects boundary conditions rather than emergent long-range physics [26, 27]. Combining the analytic  $q_{\parallel} = 0$  mode theory with molecular dynamics (MD) of water, we further obtain a simple scaling relation for the minimum slab area required to keep the 2D-mode contribution to the variance of local potential differences below a prescribed tolerance. Figure 1 summarizes these scalings.

**Uniform plane mode and sheet-dipole mapping**—We derive the scaling of plane-averaged potential fluctuations by resolving Poisson's equation into lateral Fourier modes, isolating the *uniform plane mode* ( $\mathbf{q}_{\parallel} = 0$ ), and mapping it to a variance of partial sums along  $z$ . We write positions as  $\mathbf{r} = (\mathbf{R}, z)$  with lateral coordinate  $\mathbf{R} \in \mathbb{R}^2$  and surface-normal coordinate  $z$ . The electrostatic potential  $\phi$  obeys Poisson's equation,

$$-\varepsilon_0 \nabla^2 \phi(\mathbf{R}, z) = \rho(\mathbf{R}, z), \quad (1)$$

where  $\varepsilon_0$  is the vacuum permittivity and  $\rho$  the charge density. We resolve the potential and charge by lateral two-dimensional Fourier transforms in  $\mathbf{q}$  (hereafter  $\mathbf{q} \equiv$

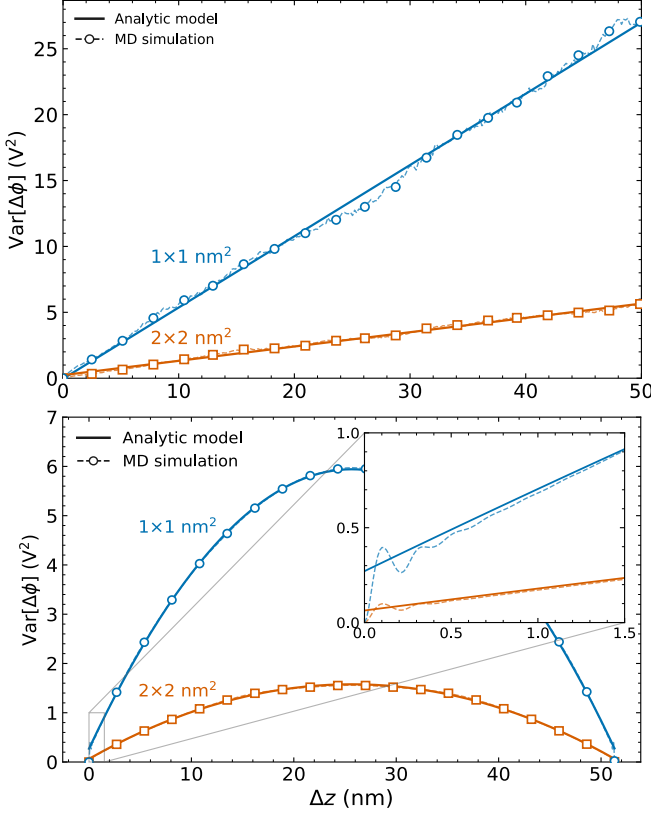


**FIG. 1. Variance of the plane-averaged electrostatic potential under 2D periodicity.** Comparing analytic theory with molecular-dynamics (MD) simulations for TIP3P water confirms the divergence of the variance in a 2D-periodic slab of a polar material of thickness 50 nm and lateral areas  $A = \{1, 4\} \text{ nm}^2$ . (a) The variance increases proportional to  $z$  away from a single electrode (random-walk behavior), and (b) follows  $z(1 - z/L)$  for confinement between two electrodes (Brownian-bridge behavior). The fitted slope  $S$  scales as  $1/A$ , isolating the uniform plane mode ( $\mathbf{q} = 0$ ), while a small constant offset  $\sigma_0^2$  captures bounded contributions.

$\mathbf{q}_\parallel$ ), without assuming any particular lateral boundary condition:

$$\begin{aligned} \phi(\mathbf{R}, z) &= \int \frac{d^2 \mathbf{q}}{(2\pi)^2} \phi_{\mathbf{q}}(z) e^{i \mathbf{q} \cdot \mathbf{R}}, \\ \rho(\mathbf{R}, z) &= \int \frac{d^2 \mathbf{q}}{(2\pi)^2} \rho_{\mathbf{q}}(z) e^{i \mathbf{q} \cdot \mathbf{R}}. \end{aligned} \quad (2)$$

In a periodic cell the same formulas hold with  $\mathbf{q}$  discretized; the equations below are unchanged. Inserting Eq. (2) into (1) yields, mode by mode,

$$\phi''_{\mathbf{q}}(z) - |\mathbf{q}|^2 \phi_{\mathbf{q}}(z) = -\rho_{\mathbf{q}}(z)/\varepsilon_0. \quad (3)$$

The uniform plane mode ( $\mathbf{q} = 0$ ) yields the plane averages,  $\bar{\phi}(z) \equiv \phi_0(z)$  and  $\bar{\rho}(z) \equiv \rho_0(z)$ , which obey

$$\bar{\phi}''(z) = -\bar{\rho}(z)/\varepsilon_0. \quad (4)$$

With the Green's function  $G_0(z) = |z|/2$  for  $d^2/dz^2$  on  $\mathbb{R}$ , we obtain

$$\bar{\phi}(z) = -\frac{1}{2\varepsilon_0} \int_{-\infty}^{\infty} |z - z'| \bar{\rho}(z') dz' + E_0 z + \phi_0, \quad (5)$$

with constants  $E_0, \phi_0$  set by the macroscopic boundary conditions.

For any  $\mathbf{q} \neq 0$ , the solution of Eq. (3),

$$\phi_{\mathbf{q}}(z) = \frac{1}{2\varepsilon_0 |\mathbf{q}|} \int_{-\infty}^{\infty} e^{-|\mathbf{q}| |z - z'|} \rho_{\mathbf{q}}(z') dz', \quad (6)$$

decays with  $z$  with an associated decay length of  $1/|\mathbf{q}|$ . In a finite lateral cell the smallest nonzero lateral wavenumber scales as  $|\mathbf{q}|_{\min} \sim 1/L_\parallel$ , so the slowest nonuniform mode decays over a  $z$ -scale on the order of  $L_\parallel$  (e.g.,  $L_\parallel/2\pi$  under 2D periodicity).

In what follows, we focus first on systems with periodic boundary conditions parallel to the interface, for which the uniform plane mode ( $\mathbf{q} = 0$ ) extends across the entire lateral cell. This geometry is the one in which the divergence of plane-averaged potential fluctuations arises; we consider other geometries later for comparison.

To make the physical content of the uniform plane mode ( $\mathbf{q} = 0$ ) explicit, we use the standard electrostatic decomposition of the total charge density into contributions from free charge  $\rho_f$ , arising for example from mobile ionic species, and bound charge associated with the polarization density  $\mathbf{P}$  of molecular dipoles in the solvent,  $\rho(\mathbf{r}) = \rho_f(\mathbf{r}) - \nabla \cdot \mathbf{P}(\mathbf{r})$ . Under two-dimensional periodic boundary conditions parallel to the interface, the  $\mathbf{q} = 0$  (planar-averaged) charge density decomposes into corresponding free-charge and polarization contributions,  $\bar{\rho}(z) = \bar{\rho}_f(z) - \partial_z \bar{P}_z(z)$ . Substituting this form into Eq. (5) and integrating by parts yields

$$\begin{aligned} \bar{\phi}(z) &= -\frac{1}{2\varepsilon_0} \int |z - z'| \bar{\rho}_f(z') dz' \\ &\quad + \frac{1}{2\varepsilon_0} \int \bar{P}_z(z') \operatorname{sgn}(z - z') dz' + E_0 z + \phi_0. \end{aligned} \quad (7)$$

This equation describes the general relation for the plane-averaged potential  $\bar{\phi}(z)$ : free charge gives *piecewise-linear contributions* and a  $z$ -polarized dipole density gives *potential jumps*.

We coarse-grain the uniform plane mode into  $z$ -sheets of thickness  $a$  centered at  $z_n = na$  and define the sheet dipole  $p_n \equiv Aa \bar{P}_z(z_n)$ , where  $A$  is the lateral area. Approximating the  $z'$ -integral by a Riemann sum over these sheet dipoles yields, up to the linear gauge  $E_0 z + \phi_0$ ,

$$\begin{aligned} \bar{\phi}(z) &\approx \frac{1}{2\varepsilon_0 A} \sum_n p_n \operatorname{sgn}(z - z_n) \\ &\quad - \frac{1}{2\varepsilon_0} \int |z - z'| \bar{\rho}_f(z') dz'. \end{aligned} \quad (8)$$

Crossing a sheet at  $z_n$  changes  $\operatorname{sgn}(z - z_n)$  by 2, so the uniform-mode potential jump is

$$\Delta \bar{\phi}|_{z_n} = \bar{\phi}(z_n^+) - \bar{\phi}(z_n^-) = \frac{p_n}{\varepsilon_0 A}. \quad (9)$$

An analogous uniform-mode accumulation occurs for plane-averaged free charge, but we focus here on polarization fluctuations as the clean dielectric reference case.

In bulk, non-reactive water away from electrodes the plane-averaged free charge is negligible, while polarization fluctuations are intrinsic and occur on fast molecular time scales. This dielectric reference case therefore provides the cleanest setting in which the uniform-mode catastrophe is both observable and statistically well sampled in molecular simulations, before introducing the additional slow and system-dependent dynamics associated with mobile ions. A systematic treatment of free-charge fluctuations, relevant for electrolytes, molten salts, and ionic conductors, will be presented elsewhere.

Focusing on the dipolar polarization contribution, the uniform plane mode ( $\mathbf{q} = 0$ ) contribution to the plane-averaged potential can be written, via Eqs. (8)–(9), as a cumulative sum of sheet dipoles,

$$\bar{\phi}(z) = \frac{1}{\varepsilon_0 A} \sum_{z_n < z} p_n + \text{const.}, \quad (10)$$

where the additive constant fixes the potential reference (gauge).

*Stochastic increments and universal scaling*—To quantify fluctuations, we now treat the sheet dipoles  $\{p_n\}$  as a stochastic sequence generated by an equilibrium liquid. Specifically, we assume the interior sheets are (approximately) second-order stationary along  $z$ , with zero mean  $\langle p_n \rangle = 0$  and covariance

$$R_s \equiv \langle p_n p_{n+s} \rangle, \quad R_{-s} = R_s.$$

A convenient summary is the *integrated covariance*

$$R_{\text{int}} \equiv R_0 + 2 \sum_{s=1}^{\infty} R_s,$$

which is finite for short-ranged dipolar correlations, as expected for a normal bulk liquid with a finite dipolar correlation length.

For any such stationary process, the variance of the partial sum obeys the exact identity

$$\text{Var}\left(\sum_{n=1}^m p_n\right) = m R_0 + 2 \sum_{s=1}^{m-1} (m-s) R_s. \quad (11)$$

Equation (10) thus makes the uniform plane mode a partial sum of (weakly correlated) stochastic increments: in a semi-infinite slab  $\bar{\phi}(z)$  is a random walk in  $z$ , while under endpoint constraints it becomes a Brownian bridge with the same leading scaling for short-ranged correlations. Combining Eqs. (10) and (11) gives, for  $z = ma$ ,

$$\text{Var}[\bar{\phi}(ma)] = \frac{1}{\varepsilon_0^2 A^2} \left[ m R_0 + 2 \sum_{s=1}^{m-1} (m-s) R_s \right]. \quad (12)$$

For short-ranged correlations, the bracket satisfies

$$m R_0 + 2 \sum_{s=1}^{m-1} (m-s) R_s = m R_{\text{int}} + O(1) = \frac{z}{a} R_{\text{int}} + O(1),$$

where the  $O(1)$  term is a bounded contribution determined by the short-range structure of the sheet-dipole correlations. Consequently, in a semi-infinite 2D-periodic slab the variance grows linearly with depth,

$$\text{Var}[\bar{\phi}(z)] = \frac{R_{\text{int}}}{\varepsilon_0^2 A^2 a} z + \sigma_0^2 \quad (z \gg a), \quad (13)$$

$$\text{where } \sigma_0^2 = \frac{O(1)}{\varepsilon_0^2 A^2}.$$

In a finite slab of  $N$  sheets (length  $L = Na$ ) with two constant-potential electrodes or periodic boundary conditions along  $z$ , the partial sums satisfy  $\sum_{n=1}^N p_n = 0$ . For i.i.d. increments ( $R_0 = \sigma_p^2$ ,  $R_{s \geq 1} = 0$ ), the conditional variance is the standard Brownian-bridge result [28],

$$\text{Var}\left(\sum_{n=1}^m p_n \mid \sum_{n=1}^N p_n = 0\right) = m R_0 \left(1 - \frac{m}{N}\right).$$

For short-ranged correlated increments, the leading behavior is obtained by the replacement  $R_0 \rightarrow R_{\text{int}}$ , yielding

$$\text{Var}[\bar{\phi}(z)] = \frac{R_{\text{int}}}{\varepsilon_0^2 A^2 a} z \left(1 - \frac{z}{L}\right) + \sigma_0^2, \quad (0 \leq z \leq L). \quad (14)$$

The key conclusion is that the unbounded growth of the variance with slab thickness is not an intrinsic bulk material property; rather, it is a boundary-condition artifact imposed by lateral replication (2D periodicity), which injects the system-spanning uniform plane mode ( $\mathbf{q} = 0$ ). Hence, reliable conclusions from MD simulations require either suppressing/handling the  $\mathbf{q}=0$  mode or demonstrating convergence with lateral area and electrostatic boundary conditions. Since  $p_n$  is the *total* dipole of a sheet of volume  $V_n = Aa$ , its fluctuations are extensive and  $R_{\text{int}} \propto Aa$  for a bulk liquid with finite dipolar correlation length. Equations (13) and (14) then imply  $\text{Var}[\bar{\phi}] \propto 1/A$  and an RMS amplitude that scales as  $A^{-1/2}$ .

*Control geometries*—The random-walk/Brownian-bridge growth in Eqs. (12)–(14) is a consequence of the uniform plane mode injected by lateral replication. To emphasize that this behavior is not an intrinsic bulk property, we contrast it with two controls in which the potential variance saturates with distance.

*1D stack of dipolar sheets*—For a semi-infinite 1D stack of dipolar sheets separated by  $a$  (no lateral replication), the on-axis kernel decays as  $1/|m-n|^2$ . The on-axis potential at sheet  $m$  is therefore a weighted sum of all other sheet dipoles,

$$\phi_m = \alpha \sum_{n \geq 1, n \neq m} \frac{\text{sgn}(m-n)}{|m-n|^2} p_n, \quad \alpha = \frac{1}{4\pi\varepsilon_0 a^2}. \quad (15)$$

For i.i.d. sheets with  $\text{Var}(p_n) = \sigma_p^2 = \langle p_n^2 \rangle$ , this gives

$$\text{Var}[\phi_m] = \alpha^2 \sigma_p^2 \left[ H_{m-1}^{(4)} + \zeta(4) \right], \quad (16)$$

with the generalized harmonic number  $H_{m-1}^{(4)} = \sum_{r=1}^{m-1} r^{-4}$  and the Riemann  $\zeta$  function,  $\zeta(4) = \sum_{r=1}^{\infty} r^{-4}$ . Using the large- $m$  expansion  $H_{m-1}^{(4)} = \zeta(4) - \frac{1}{3m^3} + O(m^{-4})$ , one finds

$$\text{Var}[\phi_m] = \alpha^2 \sigma_p^2 \left[ 2\zeta(4) - \frac{1}{3m^3} + O(m^{-4}) \right]. \quad (17)$$

Since  $\zeta(4)$  is finite, the variance  $\text{Var}[\phi_m]$  saturates, approaching the plateau as  $1/m^3$ . Short-ranged correlations between sheets just renormalize the overall prefactor.

*Fully 3D, non periodic medium*— When the system is not laterally replicated, the dipolar potential decays as  $1/r^2$  so its square is integrable at infinity and  $\text{Var}[\bar{\phi}(z)]$  saturates to a bulk plateau as  $z$  increases away from a boundary. Equivalently, in Fourier space the plane average removes the Coulomb  $k^{-2}$  singularity: the kernel linking dipole density to  $\bar{\phi}$  vanishes as  $k \rightarrow 0$ , making the variance integrable; bulk screening further suppresses long-wavelength contributions in electrolytes [22, 23, 29, 30].

*Molecular dynamics test and variance-bound*— Equations (12)–(14) show that the variance divergence under 2D replication is an infrared effect of the uniform plane mode, which converts  $\bar{\phi}(z)$  into a partial sum of sheet dipoles. We now test these predictions against explicit molecular-dynamics simulations of water and then derive a bound for the required slab area that reduces the unphysical variance below a specified tolerance.

We perform classical MD with LAMMPS [31], using the flexible TIP3P water model with the Ewald-optimized nonbonded parameters of Price and Brooks (Model B) [32] and the standard TIP3P intramolecular geometry and flexibility of Jorgensen *et al.* [33]. Long-range electrostatics were treated with the particle-particle particle-mesh (PPPM) Ewald solver, and simulations were run in the NVT ensemble at 300 K. We simulated cells of cross section  $A = 1 \times 1$  and  $2 \times 2 \text{ nm}^2$  and length  $L \approx 50 \text{ nm}$ , collecting 100 ps of production data after equilibration.

For each snapshot we form the plane-averaged potential  $\bar{\phi}(z)$  from the  $q = 0$  Green's-function sum and then the local differences  $\Delta\phi(z_0, \Delta z) = \bar{\phi}(z_0 + \Delta z) - \bar{\phi}(z_0)$ . The reported variance

$$\text{Var}[\Delta\phi(\Delta z)] = \left\langle [\Delta\phi(z_0, \Delta z)]^2 \right\rangle_{z_0, \text{time}}$$

is fitted to the Brownian-bridge form

$$\text{Var}[\Delta\phi(\Delta z)] = S \Delta z \left( 1 - \frac{\Delta z}{L} \right) + \sigma_0^2, \quad (18)$$

where  $L$  is the cell length along  $z$ . The amplitude  $S$  captures the uniform plane mode. To leading order in slab thickness and for short-ranged dipolar correlations,

$S \simeq R_{\text{int}}/(\varepsilon_0^2 A^2 a)$ , so that  $R_{\text{int}} \propto A a$  for bulk liquids implies  $S \propto 1/A$ . It is convenient to define the area-rescaled plane-mode strength  $s_0 \equiv A S$ , which is intensive in the thermodynamic limit; to leading order  $s_0 \simeq R_{\text{int}}/(\varepsilon_0^2 A a)$ . The constant  $\sigma_0^2$  collects bounded, short-range contributions that are effectively  $\Delta z$ -independent beyond a small correlation length. Figure 1 shows that the resulting variance curves are in excellent agreement with the Brownian-bridge functional form predicted by our theory across both cell cross sections, matching the shape and magnitude within statistical uncertainty.

*Discussion*—The growth of plane-averaged potential fluctuations in 2D-periodic slabs is entirely carried by the uniform plane mode ( $q=0$ ), which is the fluctuation analogue of the Ewald surface/dipole ( $k=0$ ) term [34]. Slab-corrected 3D Ewald and true 2D Ewald schemes remove interactions between periodically repeated slabs but do not eliminate this intrinsic plane mode. The sheet-dipole mapping makes its effect explicit: at any finite lateral area it generates a random-walk or Brownian-bridge contribution to  $\text{Var}[\bar{\phi}]$  with amplitude set by  $R_{\text{int}}/A$ , whereas nonuniform modes are short-ranged in  $z$  and either vanish under full-plane averaging or contribute only a bounded background for finite-area measurements.

A variance that grows without bound with distance cannot represent a physical bulk property, since bulk phases are defined by spatially invariant thermodynamics. The divergence identified here is therefore a boundary-condition artifact imposed by two-dimensional periodicity, not a property of the material. This artificial inflation of electrostatic fluctuations propagates directly into free energies—which are configurational integrals—thereby biasing solvation, charging, and interfacial free-energy estimates even when mean electrostatic profiles appear well converged.

Consistent with this interpretation, the MD-model agreement in Fig. 1 confirms both the Brownian-bridge form [Eq. (18)] and the  $1/A$  scaling of the fitted slope  $S$  (the plane-mode strength). This suggests a simple diagnostic for existing simulations: compute  $\text{Var}[\Delta\phi(\Delta z)]$  from  $\bar{\phi}(z)$ , fit Eq. (18) to extract  $S$  and the small bounded offset  $\sigma_0^2$ , and thereby separate the uniform plane mode contribution from the short-range background.

For confined water in our geometry, the variance of a local potential difference over span  $\Delta z$  can be written as

$$\text{Var}[\Delta\phi(\Delta z)] = \underbrace{\frac{s_0}{A} \Delta z \left( 1 - \frac{\Delta z}{L} \right)}_{\text{uniform plane mode}} + \underbrace{\frac{c_0}{A_m}}_{\text{bounded floor}}, \quad (19)$$

where  $c_0 \equiv A_m \sigma_0^2$  is the area-rescaled variance floor,  $A$  is the slab area, and  $A_m$  is the measurement area (for full-plane averages  $A_m=A$ ). If the averaging is performed over a finite observation window  $A_m < A$ , nonuniform modes ( $\mathbf{q} \neq 0$ ) no longer cancel and contribute only to this bounded floor. Because each  $\mathbf{q} \neq 0$  mode is governed

by the exponentially decaying kernel in Eq. (6), this contribution remains bounded in  $\Delta z$  and does not modify the Brownian-bridge scaling of the uniform plane mode in the first term. To cap the plane-mode contribution at a fraction  $\alpha$  of the intrinsic floor requires a minimum slab area

$$A_{\text{req}}(L, \Delta z; \alpha) \approx \frac{s_0 A_m}{\alpha c_0} \Delta z \left(1 - \frac{\Delta z}{L}\right). \quad (20)$$

For flexible TIP3P water at 300 K we estimate  $s_0 \approx 0.48 \text{ V}^2 \text{nm}$  and  $c_0 \approx 0.26 \text{ V}^2 \text{nm}^2$ . Taking an *ab initio*-scale window  $A_m=1 \text{ nm}^2$ , a reactive span  $\Delta z=1 \text{ nm}$  within a  $L=3 \text{ nm}$  slab, and a 20% variance budget ( $\alpha=0.20$ ) gives  $A_{\text{req}} \approx 6.2 \text{ nm}^2$  and thus a lateral side length  $\ell = \sqrt{A_{\text{req}}} \approx 2.5 \text{ nm}$ . These numbers are lower bounds and depend on the material, force field, and boundary conditions.

*Conclusion*—Two-dimensional periodicity injects a uniform plane mode that acts as a  $z$ -integrator on the plane-averaged dipole or charge density—the essence of the  $q_{\parallel}$ -mode catastrophe. In 2D-periodic slabs this mode produces potential fluctuations whose variance grows linearly or parabolically with depth, with amplitudes that decay only as  $A^{-1/2}$  for the RMS, whereas pure 1D chains and fully 3D nonperiodic geometries exhibit bounded plateaus. The divergence of plane-averaged fluctuations in slab geometries is therefore a boundary-condition artifact intrinsic to 2D periodicity at finite slab areas, not emergent interfacial physics, and it can inflate kinetic and electrostatic-response estimates, especially in small-area polar slabs. Recognizing and quantifying the uniform plane mode  $q_{\parallel} = 0$  and using scaling relations such as Eq. (18) to choose simulation cells offers a practical route to keeping these artifacts within a chosen variance budget and to interpreting potential fluctuations as genuine material behavior.

The work was supported by the U.S. Department of Energy, Office of Science, Basic Energy Sciences, under Award DE-SC0019330, and by IPAM at UCLA under NSF Grant DMS-1925919.

---

[1] A. A. Kornyshev, *J. Phys. Chem. B* **111**, 5545 (2007).  
[2] M. V. Fedorov and A. A. Kornyshev, *Chem. Rev.* **114**, 2978 (2014).  
[3] C. Merlet, B. Rotenberg, P. A. Madden, P.-L. Taberna, P. Simon, and M. Salanne, *Nat. Mater.* **11**, 306 (2012).  
[4] D. T. Limmer, C. Merlet, M. Salanne, D. Chandler, P. A. Madden, R. V. Roij, and B. Rotenberg, *Phys. Rev. Lett.* **111**, 106102 (2013).  
[5] M. Z. Bazant, B. D. Storey, and A. A. Kornyshev, *Phys. Rev. Lett.* **106**, 046102 (2011).  
[6] R. A. Marcus, *Rev. Mod. Phys.* **65**, 599 (1993).  
[7] J. Blumberger, *Chem. Rev.* **115**, 11191 (2015).  
[8] A. Fragasso, S. Schmid, and C. Dekker, *ACS nano* **14**, 1338 (2020).  
[9] C. Dekker, *Nat. Nanotechnol.* **2**, 209 (2007).  
[10] A. A. Gurtovenko and I. Vattulainen, *J. Phys. Chem. B* **111**, 13554 (2007).  
[11] E. Spohr, *J. Chem. Phys.* **107**, 6342 (1997).  
[12] M. Stengel, D. Vanderbilt, and N. A. Spaldin, *Nat. Phys.* **5**, 304 (2009).  
[13] R. Khatib, A. Kumar, S. Sanvito, M. Sulpizi, and C. S. Cucinotta, *Electrochim. Acta* **391**, 138875 (2021).  
[14] M. T. Darby and C. S. Cucinotta, *Curr. Opin. Electrochem.* **36**, 101118 (2022).  
[15] F. Raffone, R. Khatib, M. Sulpizi, and C. Cucinotta, *Commun. Chem.* **8**, 58 (2025).  
[16] M. Buraschi, A. P. Horsfield, and C. S. Cucinotta, *J. Phys. Chem. Lett.* **15**, 4872 (2024).  
[17] C. S. Ahart, S. K. Chulkov, and C. S. Cucinotta, *Journal of Chemical Theory and Computation* **20**, 6772 (2024).  
[18] F. Deissenbeck, D. Toroz, R. Wippermann, and J. Neugebauer, *Phys. Rev. Lett.* **126**, 136803 (2021).  
[19] T. Todorova, R. Wippermann, and J. Neugebauer, arXiv preprint (2025), arXiv:2411.05925 [cond-mat.mtrl-sci].  
[20] I.-C. Yeh and M. L. Berkowitz, *J. Chem. Phys.* **111**, 3155 (1999).  
[21] A. Y. Toukmaji and J. A. B. Jr., *Comput. Phys. Commun.* **95**, 73 (1996).  
[22] S. W. de Leeuw, J. W. Perram, and E. R. Smith, *Proc. R. Soc. A* **373**, 27 (1980).  
[23] S. W. de Leeuw, J. W. Perram, and E. R. Smith, *Proc. R. Soc. A* **373**, 57 (1980).  
[24] S. Chen, C. S. Niu, and Z. Q. Li, *Phys. Rev. B* **83**, 165125 (2011).  
[25] M. Otani and O. Sugino, *Phys. Rev. B* **73**, 115407 (2006).  
[26] M. Planck, *Ann. Phys.* **4**, 553 (1901).  
[27] G. G. Stokes, *Trans. Cambridge Philos. Soc.* **9**, 8 (1851).  
[28] W. Feller, *An Introduction to Probability Theory and Its Applications*, 2nd ed., Vol. II (Wiley, New York, 1971).  
[29] J. D. Jackson, *Classical Electrodynamics*, 3rd ed. (Wiley, New York, 1998).  
[30] J.-P. Hansen and I. R. McDonald, *Theory of Simple Liquids*, 4th ed. (Academic Press, Oxford, 2013).  
[31] S. Plimpton, *J. Comput. Phys.* **117**, 1 (1995).  
[32] D. J. Price and B. R. Brooks, *J. Chem. Phys.* **121**, 10096 (2004).  
[33] W. L. Jorgensen, J. Chandrasekhar, J. D. Madura, R. W. Impey, and M. L. Klein, *J. Chem. Phys.* **79**, 926 (1983).  
[34] V. Ballenegger, *J. Chem. Phys.* **140**, 161102 (2014).